POLITECNICO DI TORINO

Scuola di Dottorato

Dottorato in ingegneria Elettronica e delle Comunicazioni

Tesi di Dottorato

SIRIO : Integrated Forest Fires monitoring, detection and decision support system with low cost commercial sensors suited for complex orography

Andrea Losso

Tutore
Prof. Giovanni Perona

Coordinatore del Corso
Prof. Ivo Montrosset

Marzo 2012

Figures Index

Tables Index

INTRODUCTION

Forest Fires in our society cause a lot of damage, in particular regarding the economic and environmental landscape. Forest fires have always been present in Italian territorial heritage, however, until the 60s (the period to which date back to the first statistics), the phenomenon has been kept within acceptable levels of impact in relation to the forest environment.

During the last 50 years, in Italy, the forest fires data collections show us an increasing from 6000 annual fires during the ’60 up to now 15000 annual fires. During this period a lot of vegetation has been destroyed and an area equal to Sicily was burnt.

In particular, during 2011, forest fires has been occurred destroying 16000 hectare of vegetation with an incrementing of 66% respect the previous year.

The causes of annual forest fires increasing are to be sought in the global climatic and socio-economic changing. In particular, the long dry season overlapping the migration from rural to urban area have led an increasing of forest fires severity.[1][2]

Wild land fires are a very prevalent disturbance on the global landscape causing many serious negative impacts on human safety, health, regional economies and global climate change .In particular, forest fires in alpine regions are even more dramatic. Complex orography environments are characterized by high spatial variability of physical parameters, hard environmental and weather conditions bearing to hard stress for monitoring hardware and efficiency and by accessibility problems strongly limiting intervention activities and damage assessment.

In the scientific landscape there are many existing project to monitor areas in order to prevent forest fires; some of these are based on remote ground station where human operators control a large portions of vegetation 24 /24 hours and 7/7 days.

Other applications are based on sensors equipped on a satellite [3] or using small UAV [4]. Both types are effective but expensive, especially when applied in automated way in a complex orography environment. In order to monitor a large portion of territory automatically, with a good cost/performances trade-off, it is necessary to develop new early warning systems. We propose a ground-based system with modular architecture, equipped with low cost commercial sensor. Our idea is to develop the software able to manage the forest fires monitoring. They allow to minimize the gap which ,the use of low cost sensors, could introduce in a remote sensing of fire hazards. A lot of software are develop using wavelet technique[5], contour based using FFT [6], neural network [7] and many other.

Our technique (see chapter 3) is based on Static and Dynamic analysis of chromatic changes between images, as Berni [8] proposed, tailored for our case of study in a large scale monitoring of vegetation and using different sensors for reduce or eliminate the false alarm rate.

Concerning the image geo-referencing tool, the present work describes an innovative projective geo-referencing algorithm able to geo-reference complex orography regions using a fixed ground station images. Besides, it does not need the collection of Ground Control Points [9][10], which is a very hard task in complex orography environments.

In order to prevent this typology of hazard, it is necessary to combine some important rules as: prevention, prediction, monitoring and early detection.

Because of that, according to our point of view, it is necessary in order to face the problem, developing engineering instruments able to contrast the deforestation caused by Forest fires. In particular, in order to optimize performances and resources operating in this framework, the Remote Sensing Group (RSG) of Politecnico di Torino developed SIRIO, an integrated monitoring system for high performance decision support.

SIRIO is built up of two main modules: the provisional model of risk forecasting and the Hardware/Software layer. This layers is subdivided in three part:

the monitoring activities, data processing algorithm of image and the decision support for user oriented.

The forecast evaluation of the fire risk has an addressing function on surveillance and monitoring activities. The monitoring system operates with low cost optical sensors scanning Visible, Near Infrared and Thermal Infrared bands and a high precision low cost moving system. The data, coming from the sensors, are sent, trough very flexible communication system, to the server station where the image interpretation algorithms work. The communication system can operate either with ADSL, GPRS standards or RF links or satellite connectivity.

The image interpretation modules process the images with innovative algorithms in order to detect the sudden irruption of forest fires on a monitored scene. The algorithms can operate in the visible, Near Infrared and Thermal Infrared domain as well. In particular, smoke detection method is developed in order to elaborate the visible images. The data-processing layers include an innovative algorithm which performs the linking of every image pixel with a geographical coordinate, latitude and longitude. The algorithm is based on projective and geometric transformation on a digital elevation model (DEM). The final products are a collection of scenario images sensed in Visible band and geo-refered which ,in case of fire severity, highlighted alarm pixels and performs the fire geographical position.

In order to make user oriented product and in order to help the operator in case the extinguish operations, a decision support tool has been developed. This tool allows to add more information layers overlapped on a Google Map. Information layers closer to the fire severity position as: helicopter landing spots, water point supply spots, access road etc. (see chapter 5).

It will be present the results during one years of monitoring campaign nearby Protezione Civile di Sanremo - Italy. SIRIO is a valuable aid in fire fight management allowing involved agencies for an efficient resources handling (both logistic and human), for finalized territory monitoring and for intervention planning oriented to operators' safety.

CHAPTER 1

1-THE SYSTEM

SIRIO system is divided in two main tasks:

- *Fire risk Prevision and Forecasting*

- *Hardware & Software Architecture*

The model developed by RSG group, FIRECAST®, generates maps highlighting the areas where the Forest Fires risk is high. The monitoring system will be placed and focused into the areas where the fire risk is relevant according to FIRECAST® model.

FIRECAST®

FIRECAST® (Corgnati et al. [11]) is a computing system for forest-fire-danger-index forecasting, which elaborates weather parameters maps to evaluate fire danger indicator on the area of interest. FIRECAST® uses as a starting point the previsional Canadian Fire Weather Index (FWI) adjusted for continental Europe latitudes and climatology according to (Viney et al. [12]), (Simard et al. [13]),Van Wagner et al. [14]), (Viney et al. [15]), (Rothermel et al. [16]) and (Nelson [17]), and adapted for alpine regions orography. The system improves the danger estimation by evaluating orographic parameters like terrain slope and orientation. Since FWI is a meteorological index, it represents fire danger levels only due to present and past weather conditions, not considering contingently human presence and actions. FIRECAST® operates on meteorological forecast input data maps, in order to obtain

output maps representing expected fire danger on examined area with forecasting time interval up to 72 hours. To compute the final indices, the method uses also the historical evolution of these quantities. As explained in (Van Wagner [16]), FWI system is composed of six codes, representing the daily changes in the moisture content of three classes of forest fuels with different drying rates, the rate of spread, the assumed fuel weight consumed and the fire intensity. In order to integrate input weather data with spatial variability information, FIRECAST® introduces correction factors related to slope (terrain inclination with respect to horizontal direction) and aspect (cardinal direction of surface's normal) in fire risk evaluation. Output fire risk is represented using four danger classes: EXTREME, HIGH, MODERATE, and LOW. An example of generated maps is shown on the figure 1.

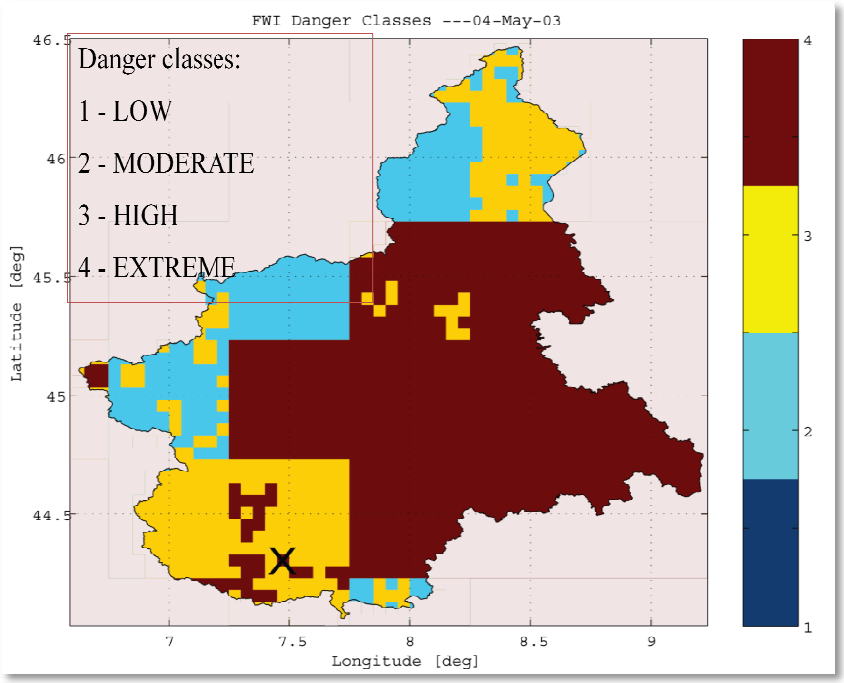

Fig.1: FIRECAST MAP

Validation results highlight the excellent capability of the system in forecasting reliable fire danger estimations and, most of all, in precise positioning of the alarm zones, with a good protection from false alarms. FIRECAST®, by evaluating combined fire risk simulation and fire statistics computation over investigated region allow the system for automatic selection of critical areas to be monitored. Furthermore, the forecast evaluation of the fire risk has an addressing function on surveillance and monitoring activities.

SIRIO SYSTEM ARCHITECTURE

The Architecture is divided into three main layers:

- *Sensor and multi-frequency monitoring*
- *Data Processing*
- *User and decision support layer*

SIRIO optimizes technological, logistic and human resources in wildfires fight assuring high performances and maximum flexibility thanks to its modular architecture based on independent operative modules and on embedded communication system. The architecture is shown on figure 2.

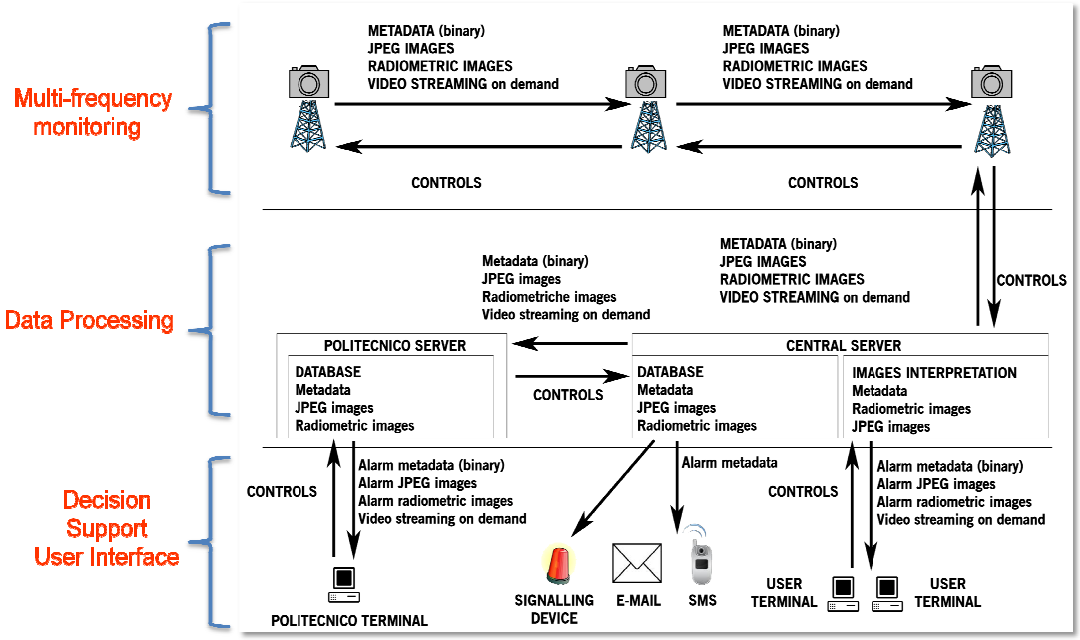

Fig.2: System Architecture

The first layer is build-up by several system, located in those areas where the FIRECAST maps show the risk; they can communicate to each other system trough internet, GPRS or WiFi connection. They are equipped with several sensor which can scan the whole monitoring area in several frequency bands. Each sensor is equipped with a computational module responsible for data acquisition and metadata integration. Acquired data are radiometric images, jpeg images, video streams, geographical metadata and weather metadata. Data and metadata are transferred to the Data Processing layer where central server runs the image interpretation software (fire risk evaluation, hot spot detection and smoke detection), the data storage, the alarms management and the decision support product generation. In the figure 3, is shown the server operational diagram.

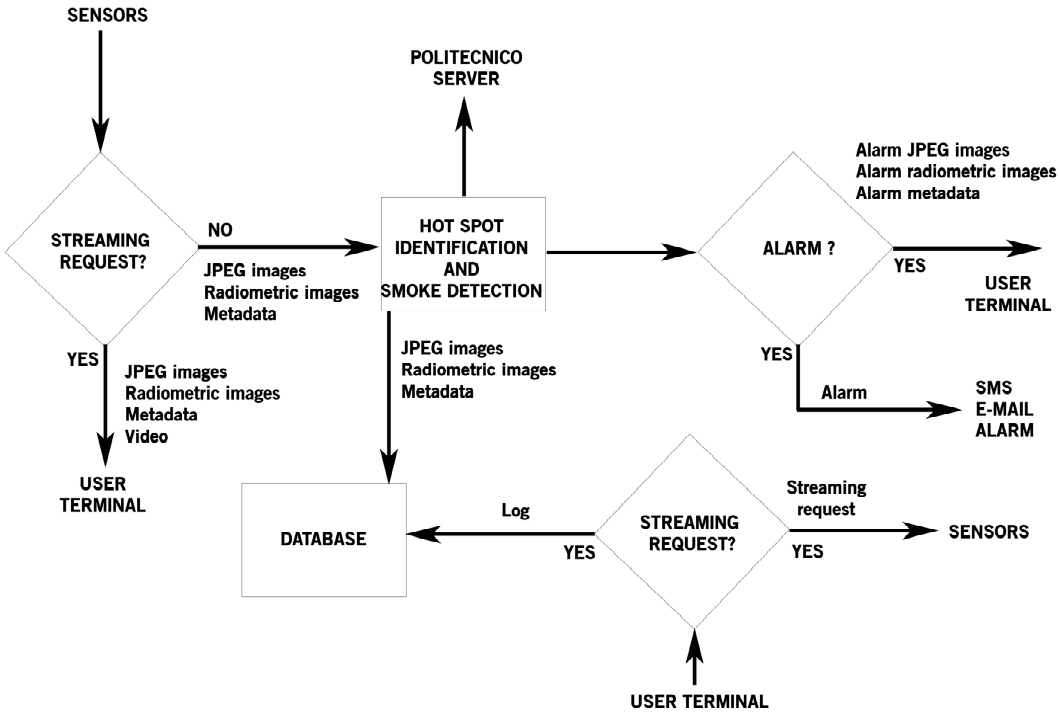

Fig 3: Server operational Diagram

The user terminals access the central server for the evaluation of statistical analysis of data stored in the database, for manual control and survey operations and for calibration and diagnostics operations. After the image interpretation, the central server sends confirmed alarms to the responsible agencies and operators as SMS messages, e-mail messages and activation of signaling devices. GUI interface are also developed in order to help the operator in case of fire severity.

The radiometric images represent the thermal distribution of the monitored scenario and are processed for the hot spot detection. Jpeg images represent the chromatic distribution of the monitored scenario and are processed for the smoke detection, for the false alarm reduction in hot spot identification and for the visualization of the monitored scenario. Metadata are ancillary information concerning local time, geographical position, sensor orientation, weather data and system operative conditions.

Sirio is installed at Sanremo (IM) as test system. The test system, is placed on the Protezione Civile' s roof fig from September 2010 up to December 2011. It generates data which are able to process to the data processing layer, where the image interpretation algorithms work. Once an alarm is found on an image, the software provides to send an e-mail to the Protezione Civile operators and to show the real time situation trough a graphic user interface (GUI).

Fig 4: Protezione Civile Building

Fig: 5 Location on google map

CHAPTER 2

2-The Architecture: Sensors & Multi-frequency monitoring

The hardware architecture is very simple and portable, as shown in the figure 6.

Fig.6 the hardware architecture

The core of the system is constituted by an engine sensors equipped, which scans the monitored scene. Monitoring scans and schedules, data acquisition, panoramic image composition and data transfer on central server are managed by the VM95® controller, a high performance, low cost, low consumption; high flexibility control system. The monitoring platform implemented in SIRIO is the Conway C995 moving system, which guarantees high performances in precision, reliability, long endurance and consumption. The moving engine operates pan and tilt movements with 0.1° precision. Monitoring sensors work onboard the moving system, protected inside IP68 cases. Cases are equipped with Gallium lenses in order to optimize the performances of sensors avoiding the flares occurrences on the lens.

The sensors acquire the data as image, according to the timing, schedule and moving of the VM95® controller. Before carried out the images is important to set some important parameter in order to obtain the data in automatically way. The parameters, as pan and tilt, are set a priori using the VM95 interface as shown in the figure 7.

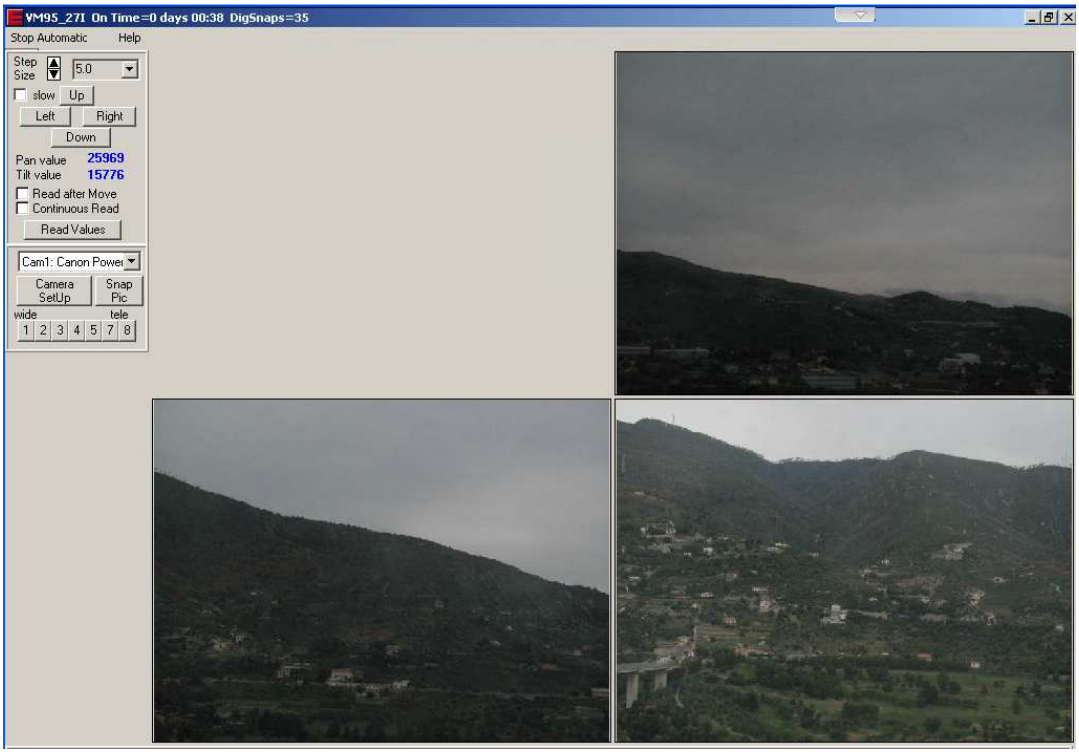

Fig 7: VM95 Interface

Pan and Tilt are the values of north orientation and horizon elevation which are necessary to set, a priori, in order to schedule the automatically position of every single picture which compose the panoramic overview (figure 8). Once, this parameters are set, the system can generates, composes and sends the panoramic overview to the data processing layers where the image interpretation algorithms work on the central server installed at Politecnico di Torino.

Fig 8: panoramic overview

SENSORS

SIRIO can be equipped by several sensor due to the modular architecture. The most important sensor that could be installed are:

- *Canon Powershot A 640* photo camera
- *Sony Block* video camera
- *Canon EOS 400D reflex* photo camera
- *FLIR A40M* thermal camera

Specifications & Characteristics

The *Canon Powershot A 640* is a low cost commercial camera (fig. 9). The Canon PowerShot A640 couples a 10 megapixel CCD imager sensor with a 4x optical zoom lens that offers a 35mm-equivalent focal range of 35 to 140mm. That's a moderate wide-angle that reaches to a somewhat more generous telephoto than you'll find on most compact cameras. Maximum apertures vary from f/2.8 to f/4.1

across the zoom range. The A640's sensor yields an ISO range of 80 to 800, with shutter speeds of 1/2,500 to 15 seconds. The parameter are listed on table 1.

Fig 9: Canon Powershot A 640

Resolution	10.00 Megapixels
CCD size	1/1.8''
Lens	4x zoom (35-140mm eq)
View Finder	Optical /LCD
LCD Size	2.5 inch
ISO	80-800
Shutter	15 -1/2500
Max Aperture	2.8
Dimensions	4.3 x 2.6 x 1.9 in. (109 x66 x 49 mm)
Weight	245g

Table 1: Camera Characteristic

The Sony Block HD, shown on figure 10, has 1280 x 720p High Definition resolution, it is suited for Security monitoring applications and it offers 1280 x 720p high definition video output. The digital LVDS interface provides easy access for IP

and Gigabit Ethernet applications. Thanks to the digital interface, the quality of the camera's video signal is maintained with minimal deterioration. This can lead to cost savings due to the direct connection to codec's/systems without the need for any additional components. The camera monitors the luminance differences within an image in high contrast environments and automatically switches on and off the Wide D feature according to the contrasted lighting environment. In addition, it is possible to select three levels of luminance differences. In the Table 2 is shown the main characteristics.

Fig.10: Sony Block Camera

Image Device	¼ type Exnor CMOS sensors
Pixels	1.450.000
Digital zoom	12x (240x with optical zoom)
Horizontal viewing angle	55.9° (wide end) to 2.9° (tele end)
Lens value	20x Optical zoom, f = 3.5 mm (wide) to 70mm (tele)
Power consumption	4.7W (motor active) 3.4W (motors inactive)
Dimensions (WxHxD)	50x 60x 89,7 mm
Weight	240g

Table 2: Sony Block Camera Characteristics

Due to the small dimensions, both video camera and photo camera can installed in the same case as shown in the figure 11.

Fig.11: Sony Block Camera & Canon Powershot A 640

The Reflex camera is used and managed by VM95 controller, *Canon EOS 400D reflex* photo camera has 10.1 megapixel CMOS sensor, a larger continuous shooting buffer, an integrated sensor vibrating cleaning system (first use in a Canon EOS DSLR), LCD with 230,000 pixels and a larger viewing angle which replaces the top status screen. The 400D uses the DIGIC II image processor. Support for the Media Transfer Protocol (MTP) USB protocol is available since version 1.1.0. The latest firmware available is version 1.1.1. The figure 12 show the camera and the table 3 show the main characteristics.

Fig.12: Canon EOS 400D

Sensor	CMOS APS-c 22.2x 12.8mm (1.6 conversion factor
Max Resolution	10.1 megapixels
Image Sensor Size	0.87 x 0.58 in./22.2 x 14.8mm (APS-C size sensor)
Lens Focal Length	1.6x
Aspect Ratio	3:2 (Horizontal : Vertical)
Color Space	Selectable between sRGB and Adobe RGB
Dimension (W x H x D)	4.98 x 3.71 x 2.56 in./126.5 x 94.2 x 65mm
Weight	200g

Table 3: Canon EOS 400D Characteristics

FLIR A40 thermal infrared cameras are FLIR long wave, handheld, Focal Plane Array cameras that are capable of temperature measurement. These camera, shown in the figure 13, is best suited for Preventive Maintenance, Research and Development, and Medical Applications. These Cameras store images on a PCMCIA Card, and the images can be analyzed using one of several available FLIR software packages (FLIR Reporter 2000 Software, Researcher 2000). The Camera can store images digitally and download those images via Fire Wire. These units are used FLIR infrared cameras. The A40M system is a complete machine vision and remote monitoring solution that can immediately identify thermal problems that are otherwise undetectable.

- Precision Temperature Measurement
- Real-Time Digital Video Output
- Multiple Target Spots & Alarms
- FireWire or Ethernet Connection Options

- Maintenance-Free Uncooled Microbolometer Technology
- LabView and C++/Visual Basic Support
- Multiple Users Can Access Data from Multiple Cameras

Fig.13: FLIR A20

FLIR cases are equipped with Gallium lenses in order to optimize the performances of the Thermal Infrared (TIR) sensor avoiding the flares occurrences on the lens.The characteristics are listed above on table 4.

System Type	Focal plane Array
Spectral Range	Long wave
Detector	320 x 240
Measurement Accuracy	+/- 2 degrees C
Measurement Range	0-15000 degree
Field of view	45 degrees
Thermal Sensitivity	<0.1 at 30 Degrees C
Camera weight	3 lbs

Table 4: FLIR A40 Characteristics

Images Generated

The system, using the sensor listed before, can composes and generates images from Visible to Thermal Infrared domain. As shown on the electromagnetic spectrum (fig 14 and table 5), it can operate from 0.4 µm to 14 µm.

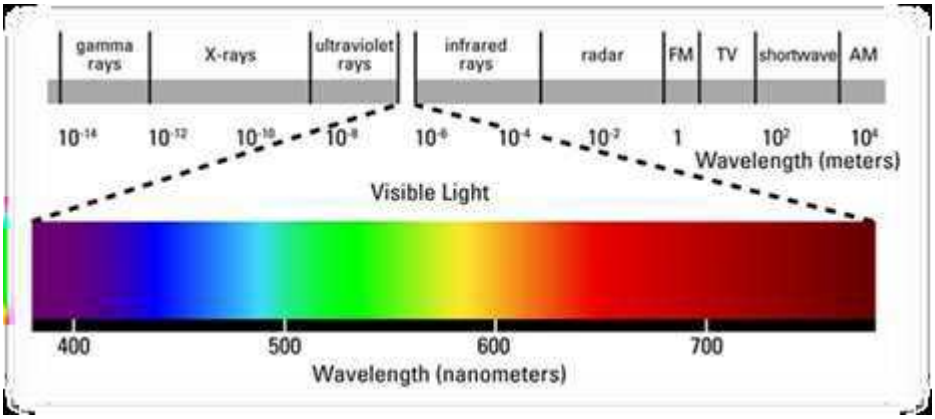

Fig.14: Electromagnetic spectrum

Bands	Wavelenght (λ)
Visible (VIS)	0.4 – 0.78 µm
Near Infrared(NIR)	0.78 µm – 1.7 µm
Medium Infrared (MIR)	1.7 µm – 6 µm
Thermal Infrared (TIR)	6 µm – 14 µm

Table 5: SIRIO Electromagnetic spectrum

SIRIO operates a multispectral scan in Visible (VIS), Near Infrared (NIR) and Thermal Infrared bands (TIR). The TIR sensing is performed with a common thermal camera. Taking advantage of the sensitivity of CCDs ([400÷1200] nm) in

both VIS and NIR bands, SIRIO mounts commercial sensors for the VIS and NIR monitoring. After the removal of the inner CC1 filters of common photo cameras and video cameras, external CC1 and IR filters are applied to the sensors for the selection of the sensing frequency band. In order to perform a monitoring activity taking into account the territory orography, video cameras and photo cameras are equipped with zoom lenses.

The images which the system can generates are shown on the images below; using the same sensor it is possible to obtain three different frequency bands: VIS (fig. 15a), NIR + VIS (fig. 15b), NIR (fig. 15c). This is an important feature of the system, because with a normal low cost commercial sensor it is possible to obtain three frequency domain at price of one sensors.

In the figure 15d is shown the panoramic overview generated by VM95 using the thermal Infrared Camera.

Fig. 15a: Reflex camera equipped with CC1 filter – Visible

Fig. 15b: Reflex camera without filters– Visible + Near Infrared

Fig. 15c: Reflex camera equipped with IR filter – Near infrared

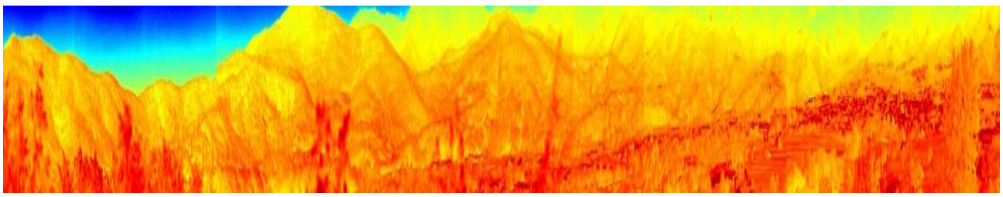

Fig. 15d: Thermal camera – Thermal Infrared

Pan & Tilt settings

The images generated by SIRIO are composed using several picture. Every single picture has a portion of the monitored scenarios, the field of view of each picture depends on the sensor used and the zoom fixed a priori.

In photography, angle of view or field of view (FOV), describes the angular extent of a given scene that is imaged by a camera. It is used interchangeably with the more general term field of view.

For lenses projecting rectilinear (non-spatially-distorted) images of distant objects, the effective focal length and the image format dimensions completely define the angle of view. Calculations for lenses producing non-rectilinear images are much more complex and in the end not very useful in most practical applications. (In the case of a lens with distortion, e.g., a fisheye lens, a longer lens with distortion can have a wider angle of view than a shorter lens with low distortion). Angle of view may be measured horizontally (from the left to right edge of the frame), vertically (from the top to bottom of the frame), or diagonally (from one corner of the frame to its opposite corner).

For a lens projecting a rectilinear image, the angle of view can be calculated from the chosen dimension (d), and effective focal length (f) as follows:

$$FOV = 2arctan\frac{d}{2f} \tag{2.1}$$

d represents the size CCD in the direction measured. As mentioned before, a commercial sensor on a digital camera, has CCD sensible to NIR+VIS wavelengths.

For example, using a Canon Powershot 640, the CCD size is 1/ 1.8". The dimension of the CCD sensor are: Height= 5.3 mm, Width = 7.17 mm and the diagonal is equal to 8.43 mm. The focal length equivalent change between 35 mm and 102 mm, it depends by the zoom selected. In our case we have two unknown quantity: the FOV of every single picture and the focal length f. In order to calculate (2.1), it is necessary to know almost one of them. In this case we obtain the FOV, setting the pan and the tilt for every single picture and with a compass we obtain the angle of the whole monitored scene (total FOV). We divide the total FOV into portion equal to the number of the picture took and we have obtained the Field of view of every single shot. In the table below are resumed the Pan and Tilt values and the north orientation for every picture which compose the panoramic overview. The orientation was taken using three different compass: classic, electronic and GPS compass. Vertical and horizontal inclinations are taken into account as well. Adding each North Orientation we calculate the total FOV.

scene	pan	Tilt	North Orientation: Classic Compass[°]	North Orientation: Electronic Compass[°]	North Orientation: GPS Compass [°]	Vertical Inclinations [°]	Horizontal Inclinations [°]
1	2233	5654	246	259	254	5,5	3
2	4556	5682	278	278	280	3,1	1,6
3	6898	5714	309	309	308	2,55	0
4	9158	5737	337	336	336	2,8	-0,3
5	1426	5766	4	3	3	3,5	1,8
6	3696	5776	29	28	29	4,6	1,7
7	5971	5780	54	55	56	5,9	-1,6

Table 6: Pan,Tilt,North Orientation, Vertical and Horizontal inclinations of Canon Powershot 640

The Pan and Tilt values are set manually in order to do not overlap the same scenario in the neighbored picture as shown in the figure 15a. Once set this values, VM95 is able to move in automated way to that positions. For every position, the north orientation and the inclinations are taken using different instruments; in the table 6 are reported the values. Using the GPS compass, the field of view starts form 254° to 56°. The average for every single picture is 27°. Since the compass target is the middle of the FOV, the total FOV stars from 254°-(27° / 2) = 240.5° to 56 + (27°/2) = 69.5°, therefore the total FOV is 189°.

From the value of the FOV, it is possible to calculate the focal length f using (2.2) and considering the dimension of the sensor d, as the width equal to 7.17 mm.

$$f = \frac{1}{2} \cdot \frac{d}{\tan\frac{FOV}{2}} \quad (2.2)$$

$$f = \frac{1}{2} \cdot \frac{7.17}{\tan\frac{27°}{2}} = 14.93 \text{ mm} \quad (2.3)$$

This value of f will be useful to calculate the vertical field of view (vFOV). Using (2.1), the height equal to 5.3 and (2.3), the vFOV will be:

$$vFOV = 2arctan\frac{5.3}{2*14.93} = 20.3° \quad (2.4)$$

Therefore, at this point we have calculated the horizontal hFOV = 27° and the vFOV = 20.3°.

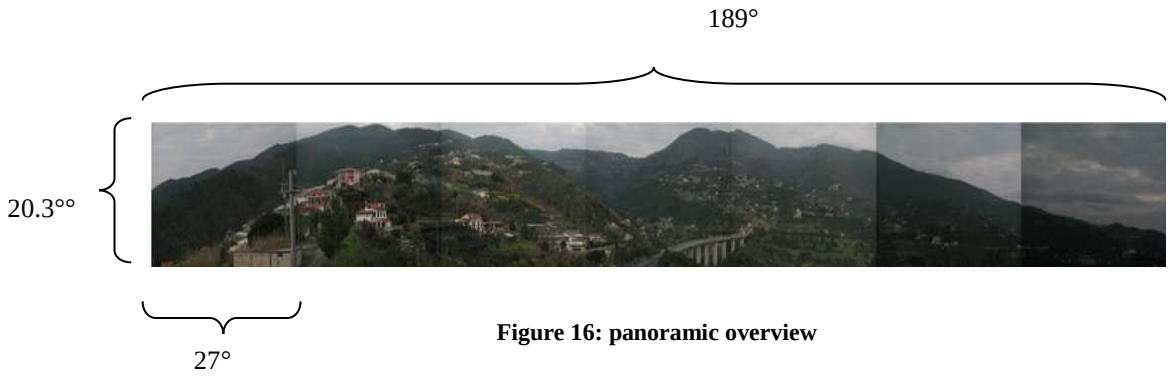

Figure 16: panoramic overview

The same procedure could be done using the Thermocamera, videocamera and the Reflex Camera. The tables below show the pan, tilt, north orientation and the inclinations related to the FLIR thermocamera.

scene	Pan	Tilt	North Orientation: Classic Compass	North Orientation: GPS Compass	Vertical Inclinations	Horizontal Inclinations
1	6458	5414	300	302	6,2	0
2	7412	5414	312	314	6,3	0
3	8375	5414	324	326	6,5	0
4	9368	5414	335	336	6,7	0,9
5	0348	5414	345	347	7,1	1,3
6	1289	5414	356	358	7,4	1,3
7	2259	5414	7	7	8,1	1,6
8	3185	5414	17	18	8,6	1,7

Table 7: Pan,Tilt,North Orientation, Vertical and Horizontal inclinations of FLIR ThermaCam

THERMAL MONITORING USING A RADIOMETRIC MODEL

In nature, all bodies whit a temperature greater the absolute zero, radiates according to the radiometry's law. In particular, if it is considered a black body, the irradiation is governed by the Plank's law. According to that it is possible to say that the magma is governed by this law as well.

A large part of energy transmitted by the magma is concentrated in a electromagnetic spectrum region between visible and thermal infrared. Using a Wien's law, it is able to estimate and calculate the value of wavelength at which the emission is maximum.

The electromagnetic spectrum is divided into several regions, ranked according to wavelength bands and named. In the electromagnetic spectrum, whole radiation are governed by the same laws and the only differences are those related to different wavelength (λ). The division of the EM (ElectroMagnetic) spectrum is shown in the table 8.

Band	Waveleght (λ)
Ultraviolet	3 nm – 0.4 µm
Visible (VIS)	0.4 – 0.78 µm
Near InfraRed (NIR)	0.78 µm – 1.7 µm
Medium InfraRed (MIR)	1.7 µm – 6 µm
Thermal InfraRed (TIR)	6 µm – 14 µm
Far Infrared	14 µm – 1 mm
Microwave	1 mm – 0.3 m

Table 8: wavelength of EM spectrum

The figure below shown us a graphical representation of the EM spectrum; enlargement is done in thermocamera sensitive region (2 ÷ 13 µm).

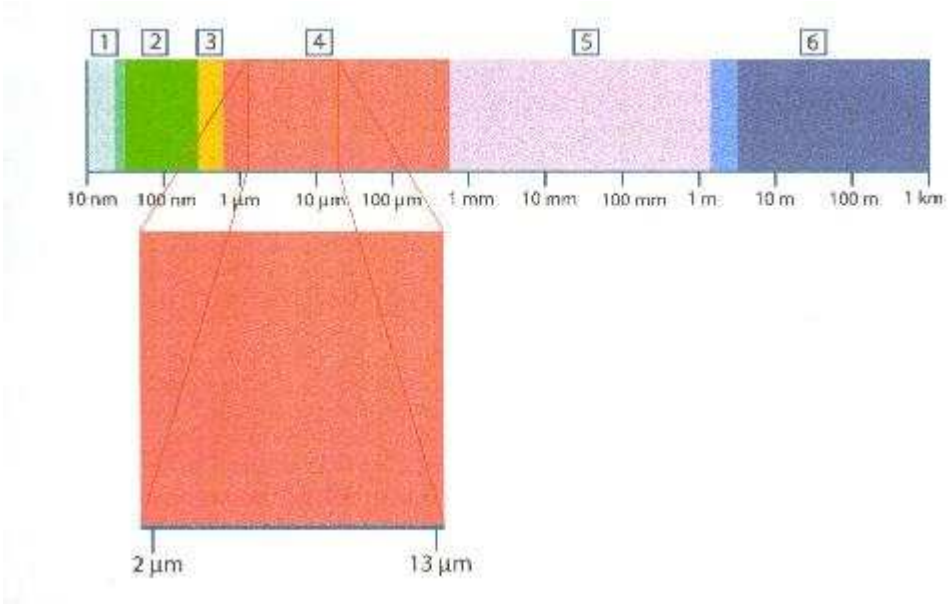

Figure 17 – EM spectrum

At this point, using the Wien's law (2.5) is possible to determine the wavelength corresponding to the magma maximum radiation.

$$T \cdot \lambda = b \tag{2.5}$$

Where $b = 2{,}897 \cdot 10^{-3}\ [mK]$. To do that, it is necessary know the forest fires temperatures shown in the table 9.

Fire Typology	Temperature [°C]	Wavelength [μm]	Spectrum
Preheating phase	100	7.77	TIR
Endothermic gas phase	160	6.69	TIR
Exothermic gas phase(wood)	350	4.65	MIR
Exothermic gas phase (flame)	1000	2.28	MIR
Solid combustion	850	2.58	MIR
Under brush fire	400	4.3	MIR
Other fire typology	600-1100	3.32 – 2.11	MIR

Table 9: Temperature of Forest fires hazard:

According to the values obtained, it is noted that all the highest emission generated Forest fires hazard are concentrated in the MIR band.

Obviously it is not true to say that all the radiation produced by these heat source are concentrated in these areas of spectrum.

It is necessary to notice that the maximum is calculated in the ideal conditions, without take into account the air conditions which could prevent the propagation of radiation at certain wavelengths.

Since these, results show that the maximum radiation is located in the infrared domain, and for this reason could be used even sensors less expensive which operate (using particular filter lens) in the infrared band such as cameras and videocameras.

ThermoCamera

In general, the thermocamera is a device which is able to detect the thermal radiations emitted by observing object. Such radiations come from environment, they are reflected from the object's surface as well. These radiations are attenuated by the atmosphere in the measuring path. Finally we must to join another radiation which come from the atmosphere itself. Dispersion sunlight in the atmosphere and external radiations are be neglected. That is described in the figure below.

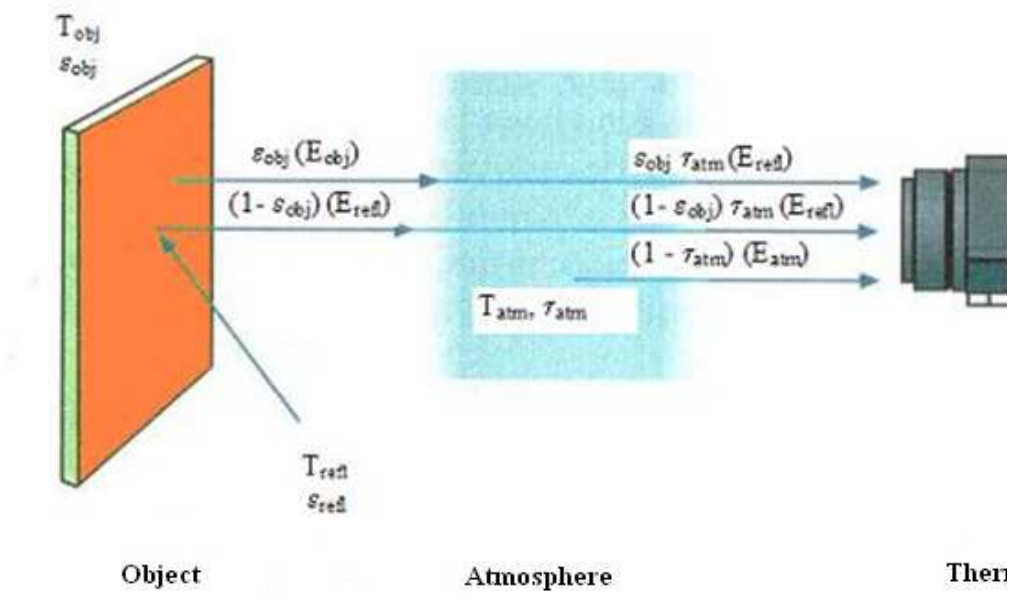

Figure 18: Irradiance contribution to the thermocamera

Considering the emissivity ε, transmittance τ, temperature T, as shown in figure 18, there are three types of irradiance contributions:

1- Emission object equal to $\varepsilon_{obj}\ \tau_{atm}\ E_{obj}$;

2- Reflected emission from the environment equal to $(1-\varepsilon_{obj})\tau_{atm}$ E_{refl} where $(1-\varepsilon_{obj})$ is the reflectance of the object:

3- Emission atmosphere equal to $(1-\tau_{atm})\, E_{atm}$ where $(1-\tau_{atm})$ is the emissivity of the atmosphere.

Considering these three terms is possible to know the general radiant energy received (E_{tot}):

$$E_{tot} = \varepsilon_{obj}\tau_{atm}E_{obj} + (1-\varepsilon_{obj})\tau_{obj}E_{refl} + (1-\tau_{atm})E_{atm} \tag{2.6}$$

Thermocamera is able to convert this Energy into a signal V_{tot}, proportional to the Energy (E_{tot})

$$V_{tot} = c \cdot E_{tot} \tag{2.7}$$

Substituting equation (3.2) in (3.3) we obtain the corresponding values of signal voltage V.

$$E_{tot} = \varepsilon_{obj}\tau_{atm}V_{obj} + (1-\varepsilon_{obj})\tau_{obj}V_{refl} + (1-\tau_{atm})V_{atm} \tag{2.8}$$

Knowing emissivity ε_{obj}, transmittance τ, the voltage signal is directly converted to a temperature. The temperature value obtained considering all three contribution of radiant Energy previously described.

Starting from forest fire models identification we developed an empiric model. To do that it is necessary to determine minimum dimensions of the forest firtes and the instantaneous field of view of thermocamera (IFOV), which represents a pixel displayed on the thermal map generated. Considering the equation 2.7, setting the atmospheric transmittance value as 0.88 (datasheet of Thermovision™

A40M, FLIR Systems) and the heat source as black body; the approximated equation became:

$$E_{tot} = 0.88 \cdot E_{obj} + (1 - 0.88) E_{atm} \quad (2.9)$$

Where E_{tot} is the total irradiance on the sensor. As shown in the equation the second term is neglected due to black body assumption and the value of τ_{obj} is equal to 1. The conversion from energy value to temperature value are made under the Stefann-Boltzaman's Law.

Once the total irradiance and the corresponding temperature T_{tot} are calculated, in order to determine the pixel temperature we consider that the sensor carries an average of all incident radiation on the pixel.

As an example, at a certain distance if the heat source observed occupies only half pixel with a temperature equal to 1000 °C and the remaining half part of the pixel is the environmental temperature set to 20 °C, the total observed value by the sensor will be 510 °C.

Using this approach, the main idea is to determine the maximum distance in which the heat source could be detected. Considering the figure shown below:

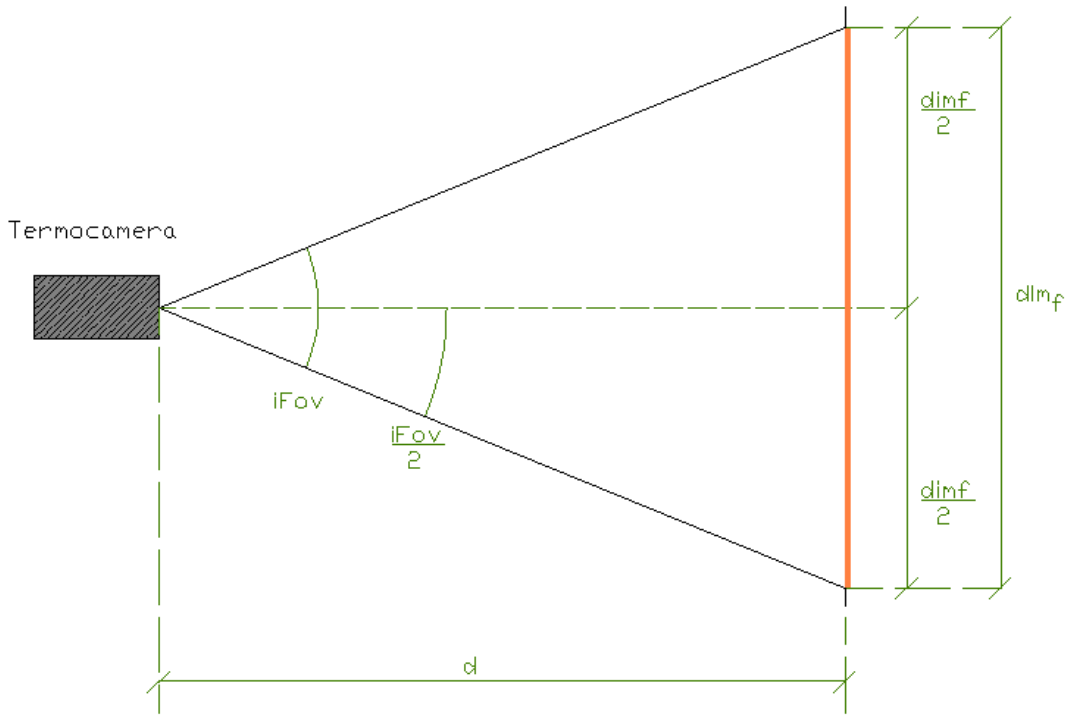

Figure 19 : maximum distance *d*

Knowing IFOV and the heat source dimension dim_f ,it is possible to calculate the maximum distance d at which the size of heat source fall entirely within a thermal map pixel.

Starting from these hypothesis it is possible to calculate the maximum distance at which the heat source will be recognized. The distance will be increased until the value temperature (measured by thermocamera) will be below to temperature threshold set a priori. This value of threshold is chosen to avoid false alarm.

The point of that is to try to model the fire and smoke coming from the forest fires according to a two dimensional geometry which models the size of the heat source in the early stage of the hazard. The value of dim_f is chosen in order to obtain the best compromise between performance, false alarm rate and missed detection.

Regarding forest fire, the flame front model is described starting from the relationship between height and width flame under the classification of (Brown and

Davis, 1973). According to this classification, the fire or generally the heat source, is classified according to various two dimensional geometry depending on the type of the observed object which we intend to identify. In order to model flame front it was thought to choose an appropriate geometry considering the external factor as rectangle due to these factors.

Since it is tried to identify and model flame front at the early stage of its process, it is important to choose the best compromise between the size dim_f and the maximum distance at which the forest fires are able to be identified.

For that reason it is analyzed different size and dimensions; changing dim_f size, change the maximum distance at which forest fire is identified as shown in the figure 20.

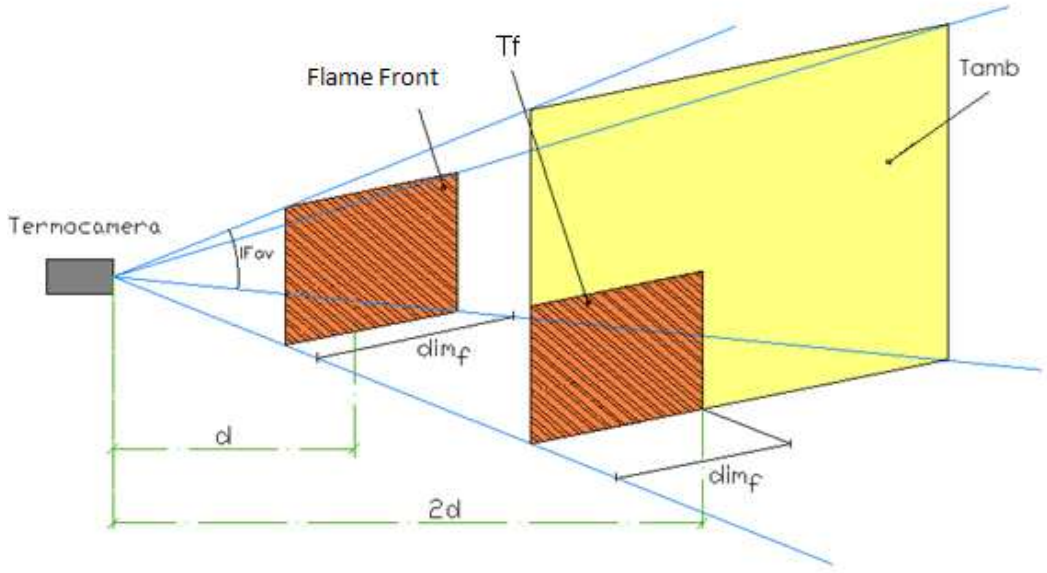

Figure 20 : model fire front

Model results

The results are shown in the figures below. Considering several two dimensional geometry, environmental temperature equal to 20 °C, threshold temperature equal to 40°C, and the Forest fires temperatures shown in the table 9; it is possible to calculate the distance *d*, and the relative temperature, at which the size of heat source fall entirely within a thermal map pixel. After which it is calculated the maximum distance for the multiple of *d* (2*d*, *3d*...) until the temperature is bigger than threshold temperature (40°C).

Forest fires Typology	T [°C]	*d* [km]	Temperature [°C] @ distance:		
			d	***2d***	*3d*
			→		
 **Subterranean Fire**	400	7.69	**No detectable**		
 **Underbrush Fire**	600	7.69	126.65	45.92	**No detectable**
	700		145.56	50.46	
	800		164.54	55	
	900		183.59	58.58	
	1000		202.69	64.17	
	1100		221.83	68.76	

 **Grass Fire**	600	15.38	72.45	**No detectable**
	700		81.71	
	800		91	
	900		100.34	
	1000		109.71	
	1100		119.12	
 **Canopy Fire**	600	76.92	154.09	**No detectable**
	700		177.87	
	800		201.73	
	900		225.66	
	1000		249.63	
	1100		**273.65**	

Table 10: model results

If we observe the model results reported on table 10, it is possible to note that the maximum distance at which forest fires could be detected starts from a minimum of 8 Km to 70 km.

Model results show us a great portable and reliable if it is located in to a strategic position and equipped with a movement technique , in this way could be monitor a big portion of vegetation.